PNAS

Supporting Information for

Doping-induced Assembly Interface for Non-Invasive in vivo Local and Systemic Immunomodulation.

Baoning Sha, Shengzhuo Zhao, Minling Gu, Dion Khodagholy, Liping Wang, Guo-Qiang Bi, Zhanhong Du*
*Zhanhong Du

Email: zh.du@siat.ac.cn

This PDF file includes:

Figures S1 to S7

Other supporting materials for this manuscript include the following:

Movies S1 to S2

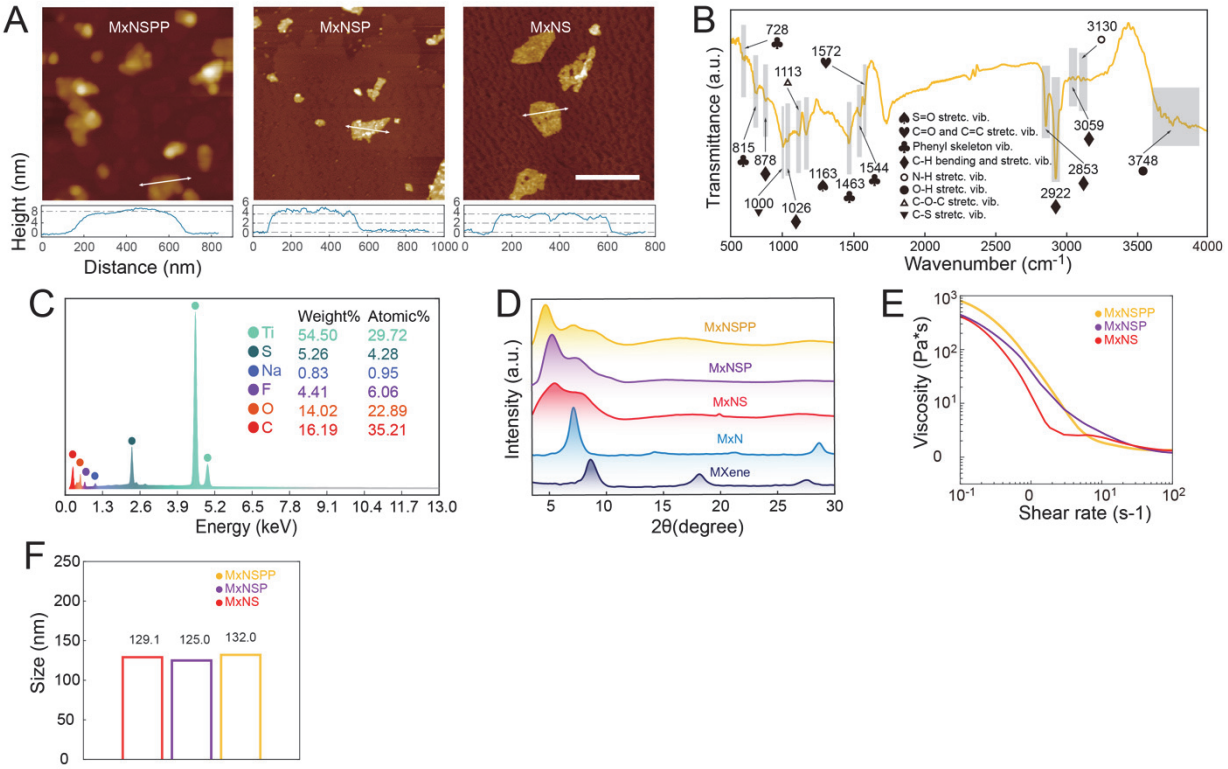

Figure S1. Characterization of nanosheets. A) Morphology and thickness of MxNSPP, MxNSP, and MxNS with atomic force microscopy (AFM) (Scale bar: 1 μm). B) FTIR spectrum of MxNSPP. C) Energy dispersive X-ray spectroscopy (EDS) of MNSPP nanosheet. D) XRD patterns of nanosheets along the synthesis process. E) Viscoelastic behavior of nanosheets (5 mg mL^{-1}) in water. F) Number-averaged size of nanosheets.

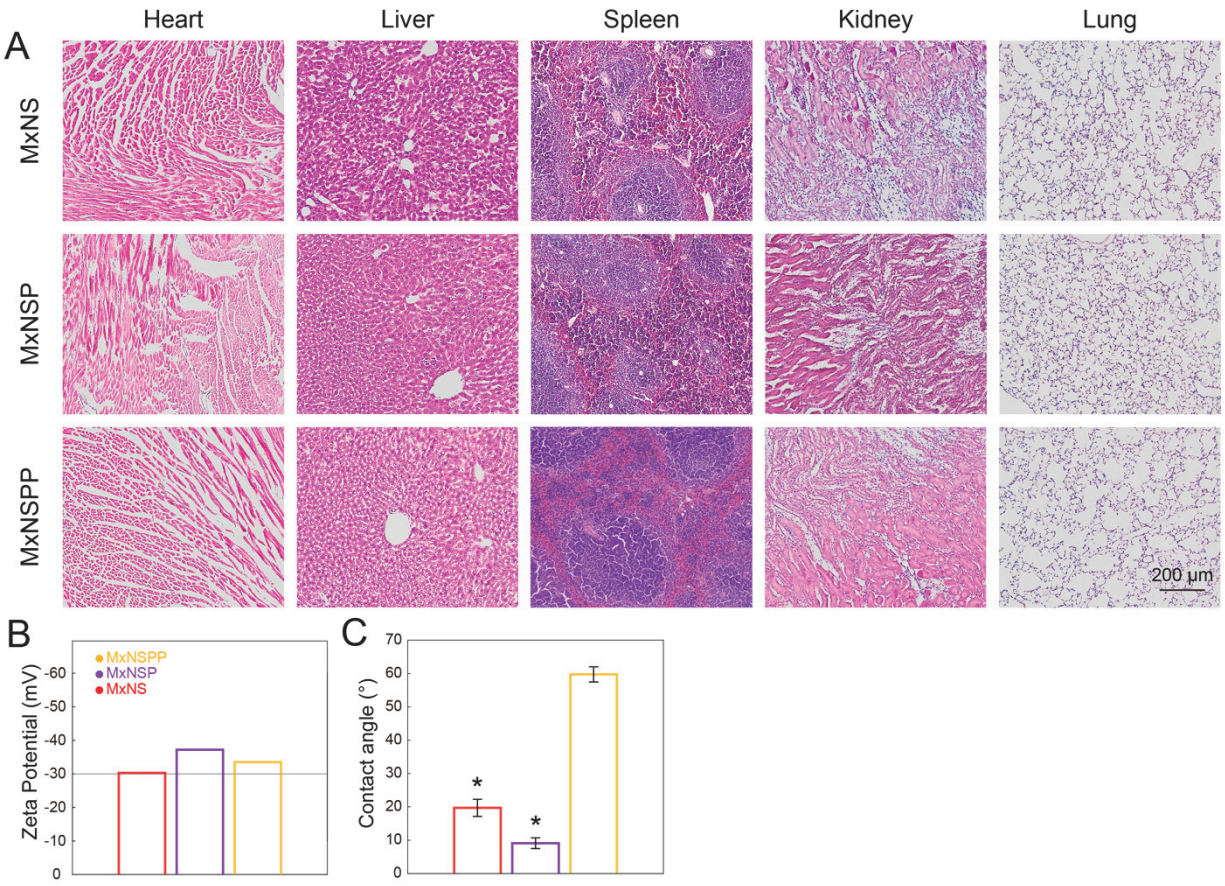

Figure S2. A) Organ toxicity of nanosheets. B) Zeta potential of nanosheets. C) Contact angle of nanosheets (n = 3). * indicates a statistical difference from MxNSPP groups ($p < 0.05$). All statistical analyses were performed by one-way ANOVA.

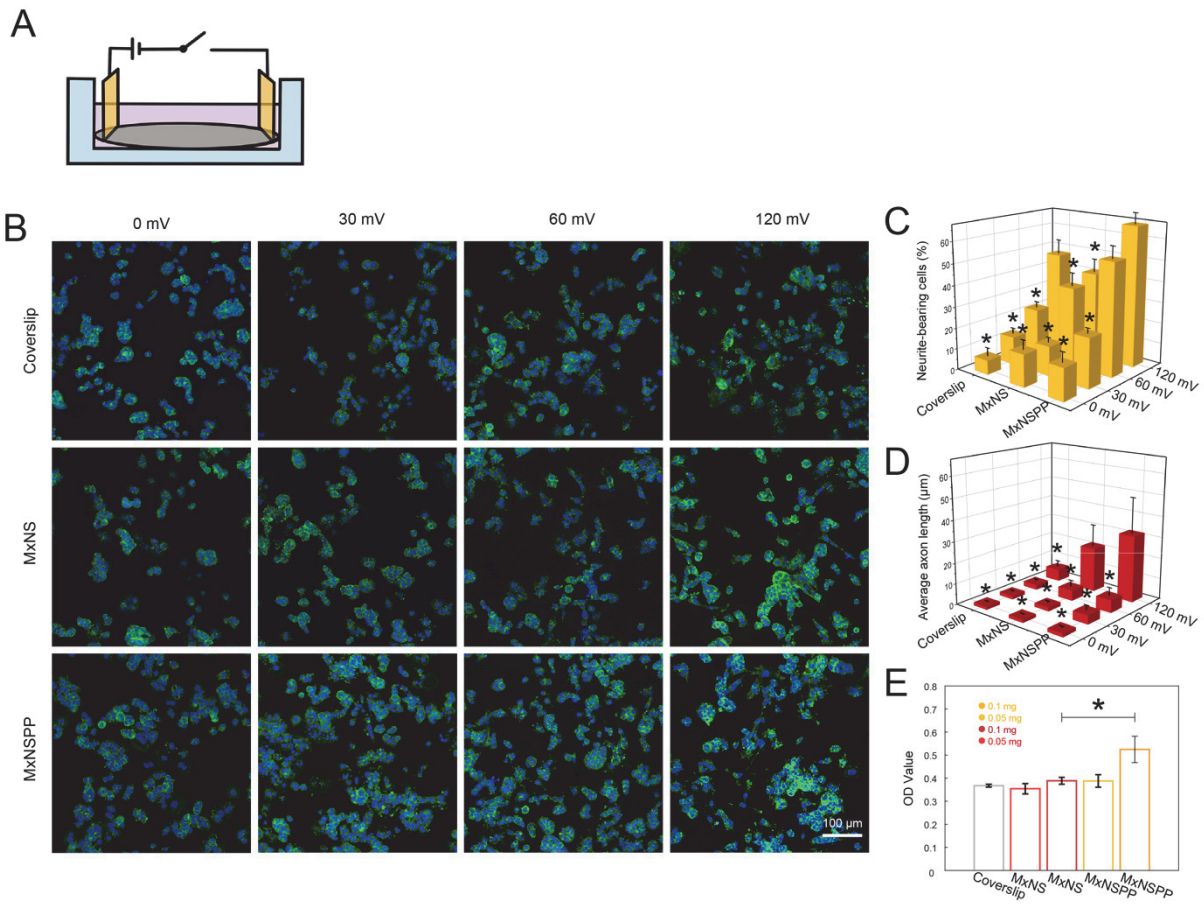

Figure S3. MxNSPP promotes PC12 proliferation and differentiation. A) Schematic representation of the cell culture device. B) Fluorescence images. C) Proportion of neurite-bearing cells. D) Average axon length of PC12 cells under different conditions (n = 3). MTT results for PC12 cells cultured on coverslips, MxNS, and MxNSPP (n = 4). * indicates a statistical difference from the MxNSPP groups of the same concentration ($p < 0.05$). All statistical analyses were performed by one-way ANOVA.

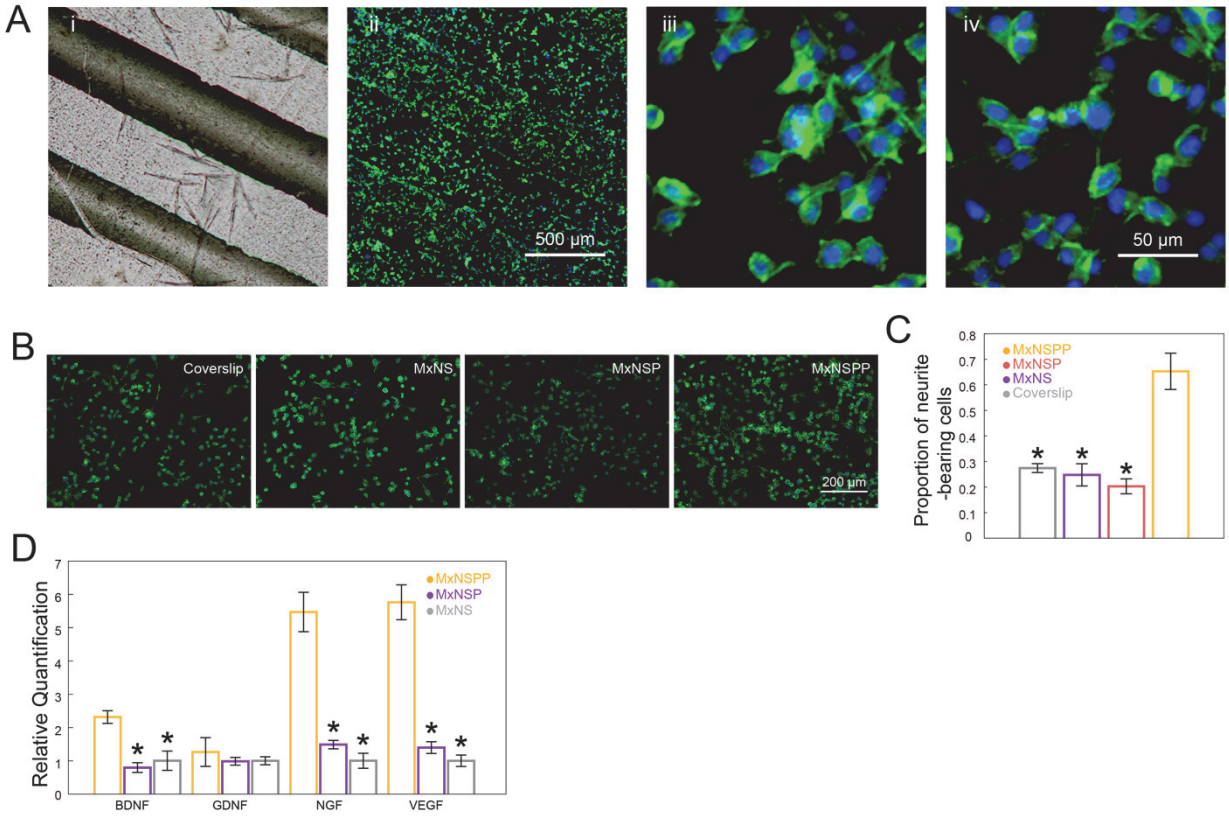

Figure S4. Characterization of nanosheet impact on cultured cells. A) Bright-field (i)and fluorescence (ii) images of SCs cultured on the MxNS pattern; fluorescence images of SCs at the gap (iii) and the grid pattern (iv). B-C) Shapes and quantitative analysis of PC12 cells in different co-culture systems with Schwann cells and nanosheets (n=3). D) qPCR analysis of Schwann cells cultured on different nanosheets (n=3). * indicates a statistical difference from the MxNSPP groups ($p < 0.05$). All statistical analyses were performed by one-way ANOVA.

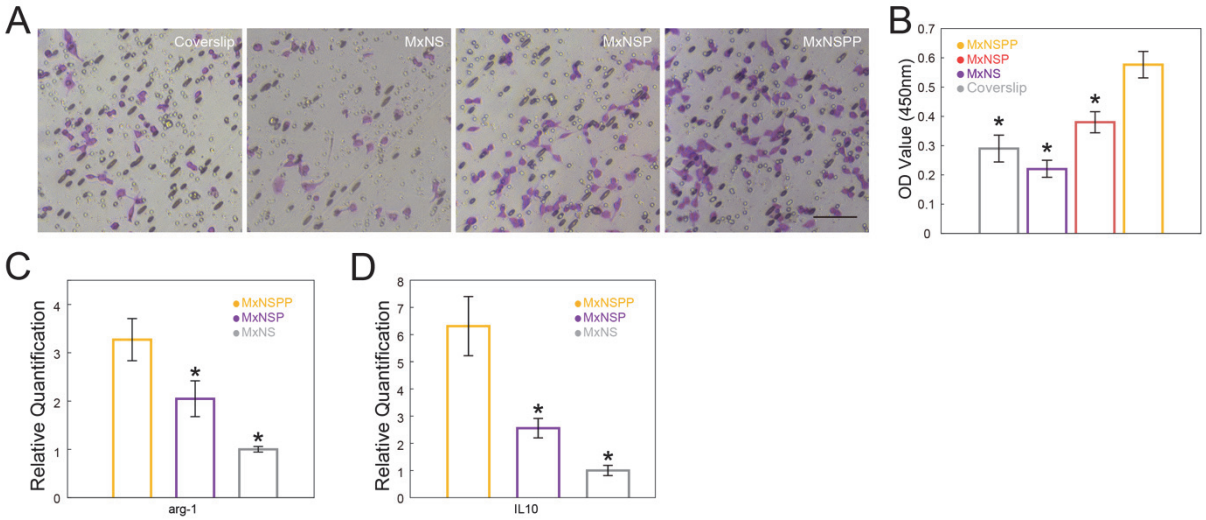

Figure S5. Characterization of nanosheet impact on cultured cells. A-B) Representative photographs and quantitative analysis of Schwan cells in different co-culture systems with

polarized macrophages and nanosheets (n=3) (Scale bar: 50 μm). C-D) qPCR analysis of gene expression associated with macrophage polarization (n=3). * indicates a statistical difference from the MxNSPP groups ($p < 0.05$). All statistical analyses were performed by one-way ANOVA.

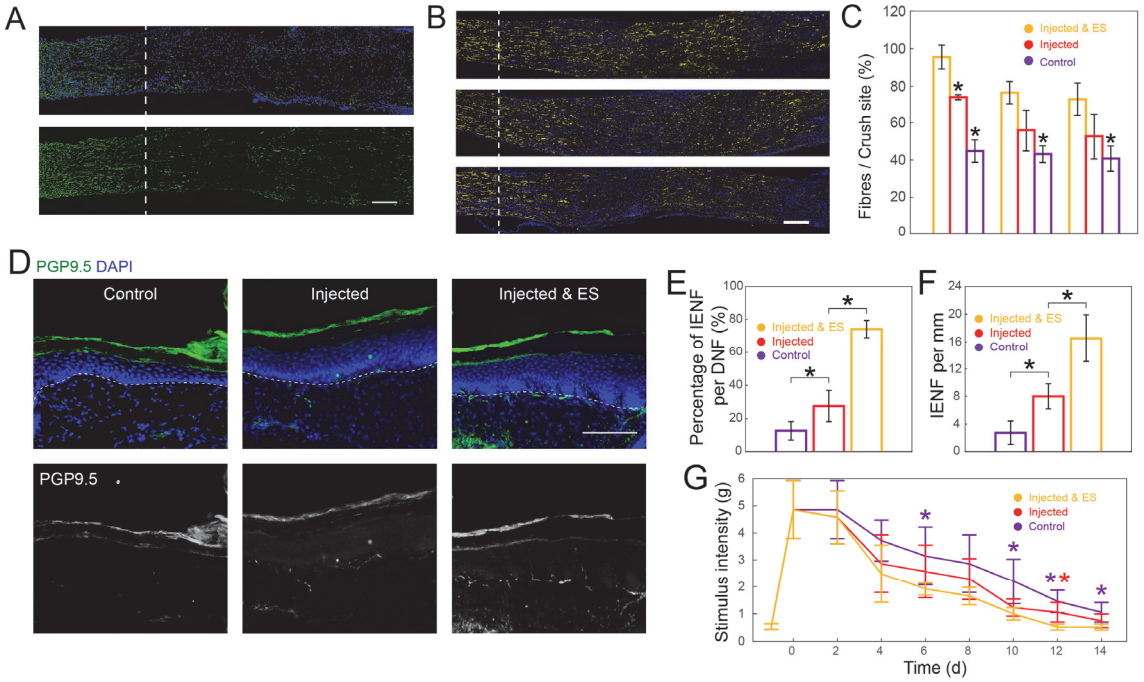

Figure S6. In vivo Characterization of jet-injected neural interface. A) Immunofluorescent images of S100+ Schwann cells in SNC representative sections before stimulation (Scale bar: 200 μm). B) Immunofluorescent images of NF200+ neurons in SNC representative sections (Scale bar: 200 μm). C) Quantitative analysis of the percentage of neurons past the crush site normalized to the fluorescence intensity at the crush site plotted as a function of the distance from the crush site (n = 3). D) Immunofluorescent images of epidermal innervation of the hindpaw interdigital skin with PGP9.5 (green) and DAPI (blue) 14 days after SNC. The dashed lines indicate the boundary between the epidermis and dermis (Scale bar: 100 μm). E-F) Quantification of the percentage of intra-epidermal nerve fibers (IENF) versus dermal nerve fibers (DNF) and the number of IENF per millimeter of interdigital skin after treatments (n = 4). G) Von Frey analysis for nociception. * indicates a statistical difference from the MxNSPP groups ($p < 0.05$). All statistical analyses were performed by one-way ANOVA.

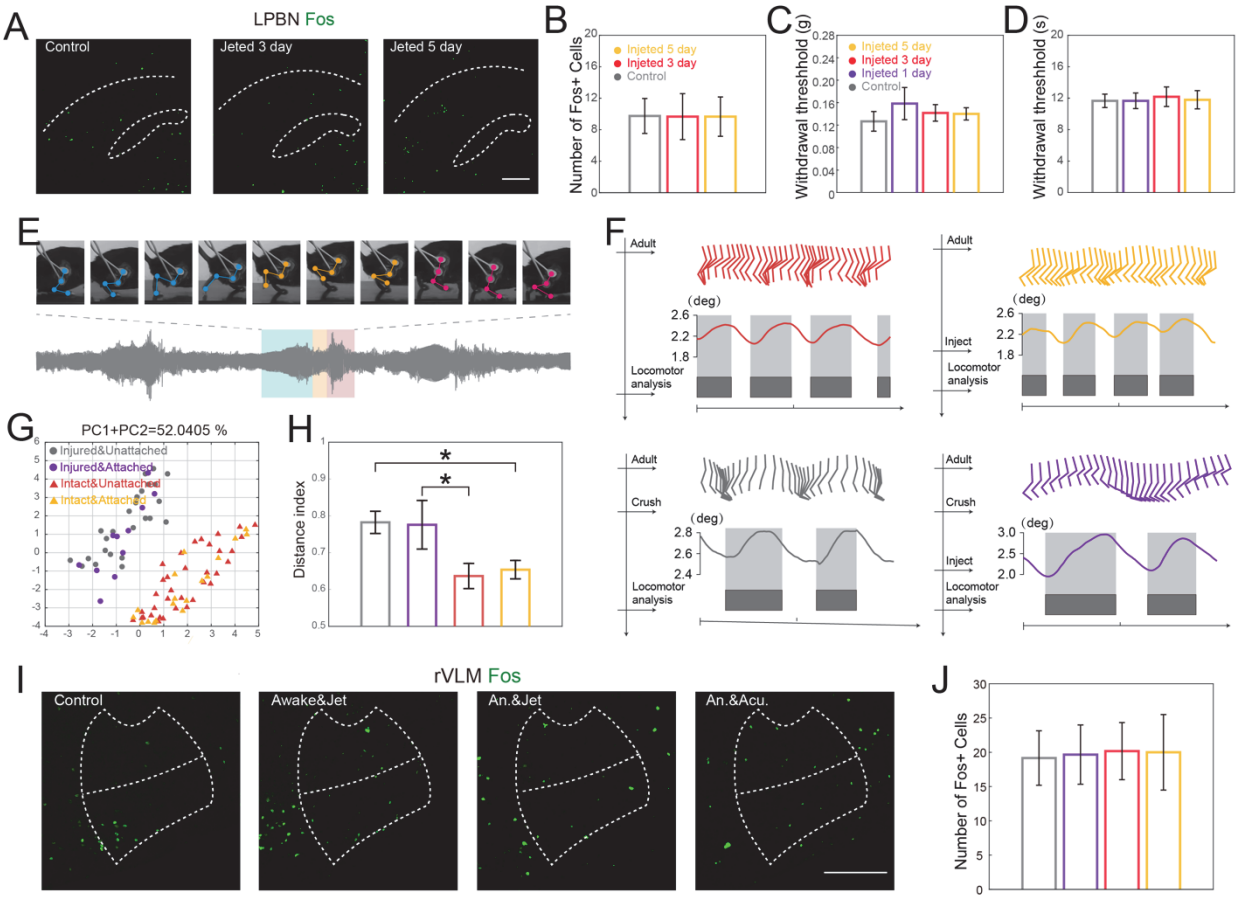

Figure S7. Behavior and pain response in mice with MxNSPP jet-injected interface. A) Immunofluorescent images of c-Fos expression (green) in LPBN after jet-injected nerve interface assembly (Scale bar: 200 μm). B) Quantitative analysis of c-Fos labeled neurons in LPBN (n = 9). b) Quantitative analysis of c-Fos labeled neurons in LPBN (n = 9). C-D) Von Frey and hot plate analysis for nociception (n = 6). E) Synchronous neural signal and joint movement recording. F) Stick decomposition, limb oscillation and corresponding stance/swing phases of different groups. Dark gray horizontal bars indicate stance, and empty spaces correspond to swing. G-H) PC analysis of different groups. Each dot represents limb kinematics of right hindlimb of one mouse. I) Immunofluorescent images of c-Fos expression (green) in rVLM following the same treatment in figure 4E (Scale bar: 100 μm). J) Quantitative analysis of c-Fos labeled neurons in rVLM in each group (n = 6). * indicates a statistical difference ($p < 0.05$). All statistical analyses were performed by one-way ANOVA.